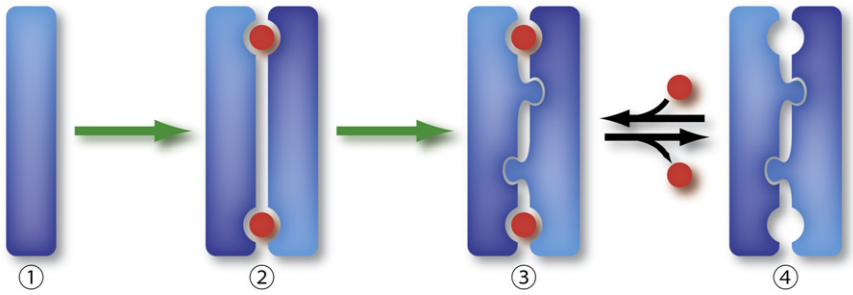

Figure 1. Outline of the Experimental Path
A non self-associating protein (1) becomes a homo-oligomer (2) through the acquisition of metal-coordinating residues at its surface. The new interface is optimized further (3) until complex formation is independent of metal-coordination (4). Metals are shown as red spheres; green arrows depict mutational events.

in early cellular environments renders it purely hypothetical.

Nonetheless, the pathway can be taken as a route to design protein interfaces as suggested, the rational approach being termed Metal Templated Interface Redesign (MeTIR). How feasible and efficient is this approach? The first step of introducing metal-coordinating residues turned out to be very effective in this case, though not entirely predictive: only one of the two designed sites led to zinc binding and in an unforeseen manner. Although a dimer was expected, a tetramer was found. A more precise prediction of metal-coordination and the resulting interfaces is desirable. Use of available computational methods for the placement of side chains with predefined geometries onto a known protein backbone might improve the accuracy of coordination site design at crystallographic interfaces. Precision is extremely important, since metal binding will be the template for the interfacial interactions to be designed. Therefore, structural studies of this intermediate construct are essential. The second part of MeTIR deals with the adaptation of the new interface, which has worked especially well for one of the interfaces in Zn:c-b562. It thus presents another good example for the successful use of the Rosetta software (Kuhlman and Baker, 2000) to optimize protein packing not only within proteins but also between them. The combination of the two steps, metal-mediated association followed by interface optimization, allows incremental improvement from a defined starting point. But one would hope that once computational protein interface design is better understood and more reliable the initial step of metal-coordination is not necessary anymore.

REFERENCES

Ambroggio, X.I., and Kuhlman, B. (2006). J. Am. Chem. Soc. *128*, 1154–1161.

Kuhlman, B., and Baker, D. (2000). Proc. Natl. Acad. Sci. USA *97*, 10383–10388.

Salgado, E.N., Faraone-Mennella, J., and Tezcan, F.A. (2007). J. Am. Chem. Soc. *129*, 13374–13375.

Salgado, E.N., Lewis, R.A., Mossin, S., Rheingold, A.L., and Tezcan, F.A. (2009a). Inorg. Chem. *48*, 2726–2728.

Salgado, E.N., Ambroggio, X.I., Brodin, J.D., Lewis, R.A., Kuhlman, B., and Tezcan, F.A. (2009b). Proc. Natl. Acad. Sci. U S A. Published online December 23, 2009. 10.1073/pnas.0906852107.

Nucleic Acid Detection using MNAzymes

Yulia V. Gerasimova[1] and Dmitry M. Kolpashchikov[1,*]
[1]University of Central Florida, 4000 Central Florida Boulevard, Orlando, FL, USA
*Correspondence: dkolpash@mail.ucf.edu
DOI 10.1016/j.chembiol.2010.02.003

Deoxyribozymes are promising biotechnological tools. In a recent *JACS* article, Mokany et al. reported on the design of multi-component deoxyribozyme (MNAzyme) sensors based on 10-23 and 8-17 DNA enzymes. The sensors can detect down to 5 pM of a specific nucleic acid. The versatility of MNAzyme platform allows the design of catalytic cascades for signal amplification. This work is a step forward to PCR-free molecular diagnostics.

The discovery of catalytic DNA molecules, known also as deoxyribozymes, DNA enzymes, or DNAzymes, by Breaker and Joyce (1994) has introduced a new versatile scaffold for the design of a variety of biotechnological tools (reviewed by Schlosser and Li [2009] and by Baum and Silverman [2008]). Sharing the advantages of biocompatibility and simplicity of structural prediction and modification with ribozymes, DNA enzymes are more stable and have lower cost of chemical synthesis than their RNA counterparts. DNAzymes have a great, though not completely explored, potential for sensing a variety of analytes (Liu et al., 2009), mainly due to the possibility of catalytic signal amplification.

Among all possible applications of DNAzyme-based sensors, the detection of specific RNA/DNA sequences is of

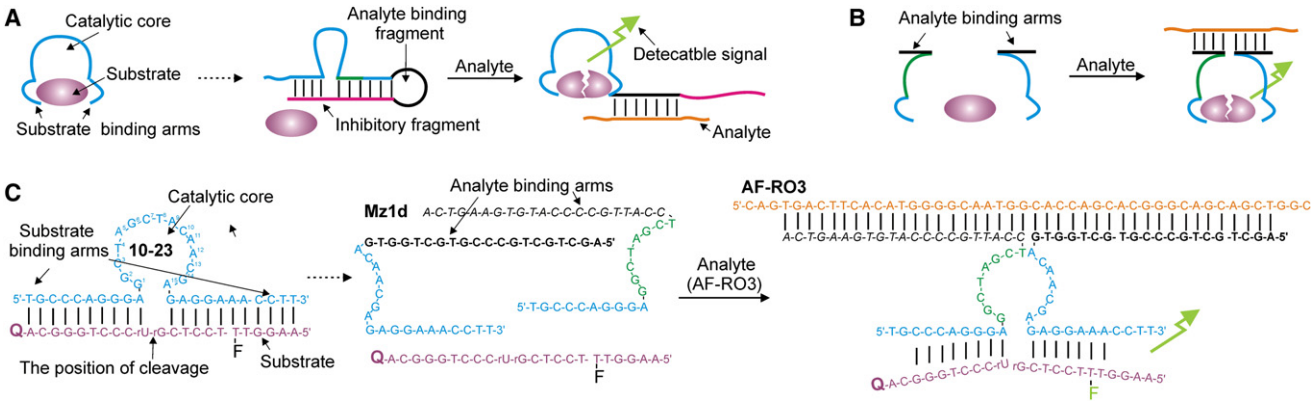

Figure 1. Design of Deoxyribozyme Sensors for Nucleic Acid Analysis
(A) Allosterically regulated deoxyribozyme sensors (e.g., Stojanovic et al., 2003).
(B) Binary deoxyribozyme sensors (e.g., Kolpashchikov, 2007, 2008).
(C) One of the MNAzyme sensors reported by Mokany et al. (2009). The enzymatic core of DNAzyme 10-23 was divided between T^8 and A^9, and the analyte binding arms (black sequences) were connected to T^8 and A^9. The presence of oligonucleotide AF-RO3 led to the formation of the catalytically active associate (right), which cleaved the fluorogenic substrate.

particularly interest because deoxyribozymes can be easily tailored to recognize these types of analytes by Watson-Crick base pairing. On the other hand, there is a need for the PCR-free assays in straightforward formats that do not require highly trained personnel and such expensive equipment as real-time PCR thermocyclers. Indeed, PCR is an ultimate in terms of sensitivity, but is relatively complex, expensive, and sensitive to contaminations. Furthermore, microarrays of deoxyribozyme sensors may enable simultaneous analysis of hundreds of thousands of analytes and thus revolutionize molecular diagnostics. Nucleic acid analysis, therefore, is the field in which the enormous potential of deoxyribozyme-based sensors can be put into practice. Recently reported MNAzyme technology (Mokany et al., 2009) takes advantage of catalytically efficient DNAzymes 10-23 and 8-17 (Santoro and Joyce, 1998) to create efficient sensors for specific nucleic acid sequences.

Selectivity and sensitivity are two major characteristics that determine the efficiency of any sensor. Choice of the proper design is a crucial step toward creating an efficient molecular sensor. Many DNAzymes share common architecture (Figure 1A, left) with a substrate binding domain and a catalytic core (cyan), which are essential to bind and process the substrate. One strategy for the sensor design uses an inhibitory fragment (magenta in Figure 1A, middle) connected to the catalytically essential nucleotides via an analyte-binding fragment (black). This fragment hybridizes to the essential nucleotides, thus preventing their interaction with the substrate. Hybridization of the analyte (orange) to the inhibitory fragment liberates the substrate-processing nucleotides and restores the catalytic activity. Active enzyme is able to multiple substrate cleavage accompanied by generating a detectable signal. This mechanism most closely resembles intrasteric regulation of natural enzymes. In this design, the analyte competes with the deoxyribozyme's essential nucleotides for binding to the inhibitory fragment. This competition may lead either to high background reaction in the absence of the analyte if the inhibited sensor structure is unstable or to the reduced sensitivity if this structure is too stable. The optimization of the length and the sequence of the inhibitory fragment can turn out to be a tedious task. In addition, such sensors are not always selective enough to distinguish analytes that differ by only one nucleotide.

An alternative strategy takes advantage of splitting the deoxyribozyme structure into two fragments (subunits), shown in Figure 1B (left). Each fragment consists of the essential substrate binding and processing nucleotides and a fragment complementary to the analyte (analyte-binding arm). Hybridization of the two subunits to the abutting positions of an analyte reunites the catalytically active core, leading to the substrate transformation followed by generation of the detectable signal (Figure 1B, right). In this approach the degree of the sensor association can be fine-tuned simply by varying the concentration of the two sensors' strands, thus completely eliminating the undesired background activity in the absence of the analyte. Moreover, the binary design enables great selectivity because each of the two short probe-analyte hybrids is more perceptive to a single base mis-paring than one long stable hybrid formed by the allosterically regulated construct shown in Figure 1A.

It has been shown that the split architecture is adoptable for deoxyribozymes, which contain either inessential for catalysis stem-loop fragments (Kolpashchikov, 2007) or G-quartets (Kolpashchikov, 2008). The present work demonstrates more general applicability of the binary design: Mokany et al. (2009) elegantly split catalytic domains of deoxyribozymes 10-23 and 8-17 to form multicomponent DNAzymes (MNAzymes). It was demonstrated that the MNAzymes can be used for sensitive nucleic acid detection in an isothermal assay or in a PCR format. For example, a 10-23-derived MNAzyme, Mz1 (Figure 1C), which demonstrated the highest analyte-dependent activation, detected as low as 5 pM DNA analyte. This limit of detection (LoD) is among the lowest reported so far for homogeneous fluorescent assays.

The LoD for enzyme-based sensors strongly depends on the catalytic efficiency of the parent enzymes. Deoxyribozyme 10-23 is the most catalytically active DNA known so far, with a k_{cat}/K_m

of $\sim 10^9$ M^{-1} min^{-1} approaching the efficiency of the "catalytically perfect" enzymes. Despite optimal binary design, the LoD of the 10-23-based sensor does not exceed picomolar range. This detection limit is not low enough to sense $\sim 10^{-13}$-10^{-16} M viral RNA found in the blood samples of infected individuals (Steininger et al., 2003). Deoxyribozyme cascades, in which the signal of a deoxyribozyme sensor is amplified by downstream reactions, can help to achieve the desired sensitivity even without PCR amplification. Such cascades were introduced by Levy and Ellington (2003) and now, in an original design, reported by Mokany et al. (2009). It has yet to be demonstrated whether DNAzyme-based cascades can improve the LoDs by 1-4 orders of magnitude to enable applications of deoxyribozyme technology in molecular diagnostics.

REFERENCES

Breaker, R.R., and Joyce, G.F. (1994). Chem. Biol. *1*, 223–229.

Baum, D.A., and Silverman, S.K. (2008). Cell. Mol. Life Sci. *65*, 2156–2174.

Kolpashchikov, D.M. (2007). ChemBioChem *8*, 2039–2042.

Kolpashchikov, D.M. (2008). J. Am. Chem. Soc. *130*, 2934–2935.

Levy, M., and Ellington, A.D. (2003). Proc. Natl. Acad. Sci. USA *100*, 6416–6421.

Liu, J., Cao, Z., and Lu, Y. (2009). Chem. Rev. *109*, 1948–1998.

Mokany, E., Bone, S.M., Young, P.E., Doan, T.B., and Todd, A.V. (2009). J. Am. Chem. Soc. Published online December 28, 2009. 10.1021/ja9076777.

Santoro, S.W., and Joyce, G.F. (1998). Biochemistry *37*, 13330–13342.

Schlosser, K., and Li, Y. (2009). Chem. Biol. *16*, 311–322.

Stojanovic, M.N., de Prada, P., and Landry, D.W. (2003). ChemBioChem *2*, 411–415.

Steininger, C., Kundi, M., Jatzko, G., Kiss, H., Lischka, A., and Holzmann, H. (2003). J. Infect. Dis. *187*, 345–351.

